Journal of Electroanalytical Chemistry 767 (2016) 84–90

Contents lists available at ScienceDirect

Journal of Electroanalytical Chemistry

journal homepage: www.elsevier.com/locate/jelechem

Highly selective dopamine sensor based on graphene quantum dots self-assembled monolayers modified electrode

Yuhui Li [a], Yingying Jiang [a], Tao Mo [a], Haifeng Zhou [a], Yancai Li [a,b,*], Shunxing Li [a,b]

[a] College of Chemistry & Environment, Minnan Normal University, Zhangzhou 363000, PR China
[b] Fujian Province Key Laboratory of Modern Analytical Science and Separation Technology, Minnan Normal University, Zhangzhou 363000, PR China

ARTICLE INFO

Article history:
Received 4 December 2015
Received in revised form 2 February 2016
Accepted 9 February 2016
Available online 12 February 2016

Keywords:
Graphene quantum dots
Self-assembled monolayers
Sensor
Dopamine

ABSTRACT

The graphene quantum dots (GQDs) were synthesized by a convenient method and immobilized to glassy carbon electrode (GCE) through covalent self-assembled method. The GQDs and the obtained (GQDs–$NHCH_2CH_2NH$)/GCE were characterized by transmission electron microscopy (TEM), Fourier transform infrared (FT-IR) spectroscopy and atomic force microscopy (AFM), etc. Its electrochemical property of the (GQDs–$NHCH_2CH_2NH$)/GCE was explored carefully by electrochemical impedance spectroscopy (EIS), cyclic voltammetry (CV) and differential pulse voltammetry (DPV). It was demonstrated that the modified electrode presents good electrical conductivity and has favorable electrochemical response to dopamine (DA). The (GQDs–$NHCH_2CH_2NH$)/GCE displays a linear range from 1 to 150 μM and a detection limit of 0.115 μM (S/N = 3) to DA, which illustrates that the modified electrode is highly sensitive towards the determination of DA. The (GQDs–$NHCH_2CH_2NH$)/GCE also possesses good anti-interference capability and well stability. Furthermore, the sensor displays satisfactory results in real samples determination which demonstrate its great potential in practical applications.

1. Introduction

Dopamine, 2-(3,4-dihydroxyphenyl)ethylamine (DA) is a neurotransmitter which plays an important role in the communication between neurons. It is linked to arrhythmia, cardiac and hypertension abnormality of dopamine concentrations [1]. Hence a simple, sensitive, and accurate analytical method for detection of DA in vivo/vitro is a subject of great importance. In the past, various methods have been developed for the determination of DA, such as spectrophotometry [2], colorimetry [3], chromatography [4] etc. Among various methods, the electrochemical method has attracted more attention due to its fast, simple, accuracy properties in recent years [5]. However, the selectivity of bare electrode is not high enough when working in the presence of other interferences, such as uric acid (UA) and ascorbic acid (AA) [6] etc. To improve the selectivity of the bare electrode, various kinds of carbon materials have been employed to modify the working electrodes, including graphene-based materials [7], carbon nanotube-based materials [8], carbon microspheres-based materials [9], nitrogen doped carbon materials [10], and so on. These carbon materials have low limit and well sensitivity to the determination of DA, but some of them are time-consuming or expensive, such as C_{60}-functionalized multiwalled carbon nanotube films [11], Laccase-si-MWCTNs composite layers [12] and tyrosinase-SWNTs-Ppy/GCE [13] etc. Therefore, it is essential to explore a suitable material that not only has good selectivity to the determination of DA but also is easy to access, atoxic and practical.

Graphene quantum dots (GQDs) are zero-dimensional with lateral size less than 100 nm and consisted of a single layer or few-layer of carbon atoms in a closely packed honeycomb structure [14]. They are a kind of fragments of graphene, thus not only have the excellent performance of graphene, such as good biocompatibility, suitable conductivity, and low toxicity etc. [15,16], and the GQDs also exhibit new phenomena due to quantum confinement and edge effects. Therefore, GQDs have received more attention recently. The application of GQDs mainly focused on the fields including photovoltaic devices [17], cellular imaging [18], drug delivery [19] and a new generation of detection [20]. Nowadays, many researchers have devoted their efforts to explore sensing systems for biological molecule. For example, Zhao et al. [21] demonstrated that GQDs modified pyrolytic graphite electrode coupled with probe single-stranded DNA for the sensitive and selective detection of various target molecules; Razmi and Mohammad-Rezaei [22] have further developed a new, simple and low cost glucose biosensor based on glucose oxidase–GQDs/GCE; Liu et al. [23] studied GQDs-based fluorescent probe for sensitive and low-cost detection of ascorbic acid; Zhang et al. [24] GQDs/gold electrode and its application in living cell H_2O_2 detection, and so on. However, there still has large developing space of the GQDs in electrochemical sensing application. Based on structure properties and oxygen-containing groups (hydroxyl, carboxyl) [19] of the GQDs, as an alternative strategy, it comes to be a good idea forming self-assembled films with chemical modification, which can further utilize the electrochemical activity of GQDs.

* Corresponding author at: College of Chemistry & Environment, Minnan Normal University, Zhangzhou 363000, PR China.
E-mail address: liyancai@mnnu.edu.cn (Y. Li).

http://dx.doi.org/10.1016/j.jelechem.2016.02.016
1572-6657/

The self-assembled technique is a popular method which employs a variety of secondary molecular interactions to form complicated multifunctional nanostructured molecular films on any surface [25]. The self-assembled monolayers (SAMs) have conformal ultrathin films and high tunable surfaces which display a better mass transport, electrocatalysis and surface area for well sensitivity, selectivity and high detection ability [26]. During the self-assembled process, secondary molecular interactions such as covalent bond [27], electrostatic interaction [19], Van der Waals and coordination interactions [25] were employed to form nanostructured molecular films. Regretfully, these films have poor stability and reproducibility in electrochemistry application because of the loose interactions like electrostatic adsorption or hydrophobic interaction. However, the rich oxygen-containing groups of GQDs will be easy to form a steady and strong covalent bond. So the GQDs can be used as an appropriate candidate for preparing self-assembled monolayers and then to construct electrochemical sensor.

In this paper, the GQDs were synthesized by convenient method and characterized carefully. Then the GQDs monolayers were obtained by self-assembled method based on amide covalent bond formed between GQDs and ethylenediamine. The GQDs self-assembled monolayers were characterized using AFM images and FT-IR spectra. The electrochemical properties of the GQDs modified electrode were deep studied by electrochemical impedance spectroscopy (EIS), cyclic voltammetry (CV) and differential pulse voltammetry (DPV). The obtained modified electrode exhibits good electrochemical response to DA, and it also shows excellent selectivity and stability for the determination of DA.

2. Experimental

2.1. Reagents and apparatus

N-hydroxysuccinimide (NHS) and 1-ethyl-3-(3-dimethyllaminopropyl) carbodiimide hydrochloride (EDC) were purchased from Yanchang Biotechnology Co., Ltd. (China). UA, AA and DA were obtained from Sinopharm Chemical Reagent Co., Ltd. (Shanghai, China). All other chemicals were analytical reagent grade and were used without further purification. Phosphate buffer solution (PBS) was prepared by mixing 0.1 M NaH_2PO_4 and 0.1 M Na_2HPO_4. All solutions were prepared with redistilled deionized water.

The transmission electron microscopy (TEM) was performed on a FEI Tecnai G2F20 electron microscope and operated at 200 kV with the software package for automated electron tomography. The surface morphology of the modified and the unmodified glassy carbon electrode (GCE, 3 mm diameter) were characterized by atomic force microscopy (AFM, CSPM5500, China). Fourier transform infrared spectroscopy (FT-IR) was recorded on a Bruker IFS66V FT-IR spectrometer. The UV–Vis absorption was recorded by a Mapada UV-1800PC (Shanghai China). Electrochemical experiments were performed with a CHI 660C electrochemical workstation (Shanghai Chenhua Instruments Co., LTD) with a conventional three-electrode system, the modified or unmodified GCE was used as the working electrode, the Pt wire and Ag/AgCl (3.0 M KCl) electrode were used as the counter and reference electrode, respectively.

2.2. Synthesis of GQDs

The GQDs were prepared according to the reported method [28]. Firstly, 2 g citric acid (CA) was put into a 100 mL beaker and then heated to 200 °C using a heating mantle. About 5 min later, the CA was liquated. Following, the color of the liquid changed from colorless to pale yellow, and then orange in 30 min, which implied the formation of GQDs. And then, 10 mg/mL NaOH solution was added into the obtained orange liquid drop by drop under vigorous stirring until the pH of the GQDs solution is up to 8.0. Lastly, the GQDs were dialyzed for 48 h with the dialysis membranes of 1000 cutoffs, and after vacuum freeze drying, the GQDs were stored at 4 °C for using.

2.3. Fabrication of the SAMs GQDs modified electrode

The GCE was sequentially polished with 1.0 μm, 0.3 μm, and 0.05 μm alumina powder and then washed successively with distilled water, ethanol and distilled water each for 1 min, and dried in nitrogen before use. The pretreated GCE was first carboxylated in 20 mM $KMnO_4$ solution containing 2 M H_2SO_4 for 30 min, then immersed in mix solution containing 6.0 mg/mL EDC and 9.0 mg/mL NHS for 1 h, and then kept in ethylenediamine for 1 h, finally dropped 10 μL 2 mg/mL GQDs on the GCE and dried in air. The GQDs were first active by mix solution containing 6 mg/mL EDC and 9 mg/mL NHS for 20 min. The obtained modified electrode was described as (GQDs–$NHCH_2CH_2NH$)/GCE.

3. Results and discussion

3.1. Characterization of the synthesized GQDs and the (GQDs–$NHCH_2CH_2NH$)/GCE

The synthesized GQDs were characterized by TEM, UV–Vis and fluorescence spectra. As shown in Fig. 1A, the GQDs display a small size with diameters about 3–5 nm from the TEM image. According to the UV–Vis absorption spectrum (Fig. 1B), a strong UV–Vis absorption band appears at around 362 nm which is consistent with the previous reports of GQDs [19]. Meanwhile, the fluorescence spectra in Fig. 1B shows that the emission wavelength of GQDs aqueous solution is excitation independent, with the fluorescence excitation and emission wavelengths at 367 and 468 nm, respectively. Fig. 1C shows FT-IR spectra of the GQDs (a) and the (GQDs–$NHCH_2CH_2NH$)/GCE (b). The FT-IR spectra of GQDs appeared absorption of stretching vibration O–H at 3418 cm^{-1}, stretching vibration of C═O at 1611 cm^{-1} and 1395 cm^{-1}, which should be ascribed to the flexure vibration of C–OH [29]. This demonstrates that the GQDs were rich in oxygen groups (hydroxyl, carboxyl). As shown in curve b of Fig. 1C, the FT-IR spectra of the (GQDs–$NHCH_2CH_2NH$)/GCE appeared the stretching vibration O–H at 3356 cm^{-1}, C═O at 1632 cm^{-1} (amid I), C–N at 1243 cm^{-1} (amid II), N–H at 1123 cm^{-1} (amid III), which proved the amide covalent bond were formed successfully between carboxyl groups of GQDs and ethylenediamine.

The morphology of the bare GCE and the GQDs SAMs were characterized by AFM, as shown in Fig. 2. The surface of the bare GCE is relatively smooth with an average roughness of 0.837 nm (Fig. 2A); but the AFM image of the GQDs SAMs shows irregular islands with an average roughness of 6.27 nm (Fig. 2B). Therefore, from the roughness change of the electrode surface, we can conclude that the GQDs were successfully assembled to the GCE surface.

3.2. Electrochemical impedance spectroscopy characterization

Electrochemical impedance spectroscopy (EIS) was used for investigation of the impedance changes in the electrode modified process. The EIS spectrum has two parts included semicircular part and linear part. The semicircular part at higher frequency corresponds to the electron transfer limited process, and its diameter is equal to the electron transfer resistance (Rct). Fig. 3 shows the EIS of the bare GCE (a), the carboxylated GCE (b), the $NHCH_2CH_2NH$/GCE (c) and the (GQDs–$NHCH_2CH_2NH$)/GCE (d) in 0.1 M KCl electrolyte solution containing 0.1 mM $Fe(CN)_6^{4-/3-}$. It is clearly observed that the bare GCE (curve a of Fig. 3) exhibits a small Rct. After carboxylated and further modified with ethylenediamine, the diameter of the semicircular part at higher frequency in the EIS increased, suggesting the obvious increase of the Rct, as shown in curves b and c of Fig. 3. However, after modified with GQDs, the diameter of the obtained (GQDs–$NHCH_2CH_2NH$)/GCE decreased obviously which means the smallest Rct (curve d of Fig. 3), this demonstrates that the existence of GQDs could decrease the resistance of the sensing platform in the solid and solution interface. This

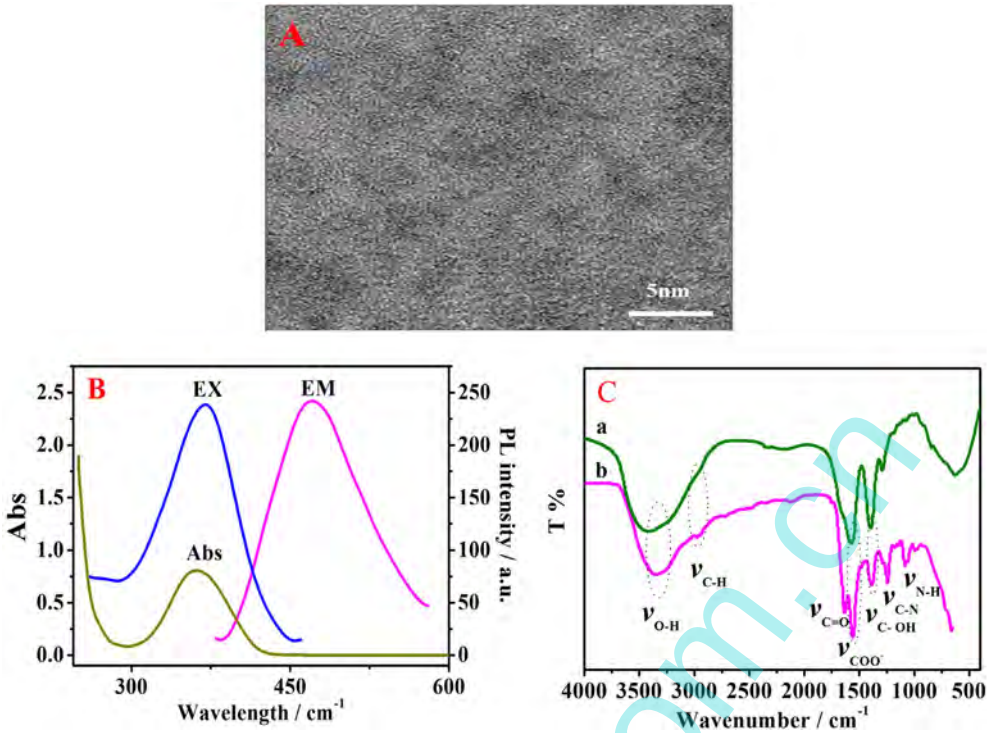

Fig. 1. (A) TEM image of the synthesized GQDs; (B) UV–Vis absorption and fluorescence spectra (Ex, Em) of the GQDs; (C) FT-IR spectra of the GQDs (a) and the (GQDs–$NHCH_2CH_2NH$)/GCE (b).

also strongly proved that the (GQDs–$NHCH_2CH_2NH$)/GCE could be a promising electrochemical platform for sensing.

3.3. Electrochemical behavior to DA

CV was used to study the electrochemical behavior of the (GQDs–$NHCH_2CH_2NH$)/GCE to DA. Fig. 4 shows the CVs of different electrodes in 0.1 M pH 7.0 PBS without and with 0.1 mM DA respectively. From Fig. 4, no redox peaks are observed for the bare GCE (curve a) and the (GQDs–$NHCH_2CH_2NH$)/GCE (curve b) in 0.1 M PBS without DA. After added 0.1 mM DA, a pair of small redox peaks appears at the CV of the bare GCE (curve c of Fig. 4) with anodic peak (E_{pa}) and cathodic peak (E_{pc}) at 0.206 V and 0.045 V, respectively. However, the CV of the (GQDs–$NHCH_2CH_2NH$)/GCE (curve d of Fig. 4) exhibits a pair of well-defined redox peaks with E_{pa} and E_{pc} at 0.170 V and 0.083 V, respectively, which indicates that a quasi-reversible electrochemical redox reaction of DA took place on (GQDs–$NHCH_2CH_2NH$)/GCE. Furthermore, the ΔE decreases from 0.161 V at the bare GCE to 0.087 V at the (GQDs–$NHCH_2CH_2NH$)/GCE, this demonstrates that the (GQDs–$NHCH_2CH_2NH$)/GCE displays better electrochemical behavior to DA. The probably reaction process may be the (GQDs–$NHCH_2CH_2NH$)/GCE adsorbed DA by electrostatic interaction, then the oxidation–reduction of DA takes place when the current generated. The possible redox mechanism of DA on the (GQDs–$NHCH_2CH_2NH$)/GCE is shown in Scheme 1. The electrochemical reaction can be ascribed to the structure of DA, a catecholamines with diols, amine functional groups and phenyl, which shows acidic with positive charge [9]. The well redox reaction of DA at the GQDs modified GCE can be attributed to the fact that the GQDs possess high electroactive surface area, good electrocatalytic activity and low charge transfer resistance, which can accelerate the electrochemical reaction of DA. Furthermore, the synthesized GQDs possess rich carboxyl groups with negative charge [19], which can attract the positively charged amine group of DA (pKa = 8.87) to the (GQDs–$NHCH_2CH_2NH$)/GCE surface through π–π bonding and electrostatic interaction. Therefore, the (GQDs–$NHCH_2CH_2NH$)/GCE have high electrochemical response to recognition of DA. Additionally, the AA (pKa = 4.1) and UA (pKa = 5.75) are repelled by the working electrode with negatively charged which can improve the selectivity of DA. The schematic illustration of the reaction mechanism of DA on the GQDs–$NHCH_2CH_2NH$/GCE was described as Scheme 1.

In addition, the effect of the GQDs concentration in preparation the (GQDs–$NHCH_2CH_2NH$)/GCE was investigated by the CVs in the presence of DA in Fig. 5A. The concentrations of GQDs were varying from 1.0, 1.5, 2.0 to 2.5 mg/mL. The results from Fig. 5B show that the oxidation and reduction peak currents of DA increased greatly with the increasing of concentration of GQDs, but the oxidation peak current reached a

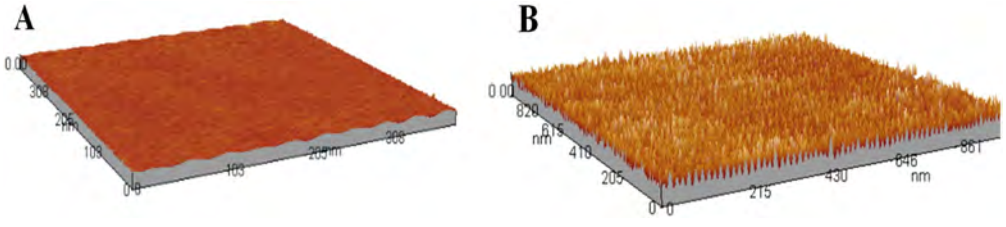

Fig. 2. AFM images of the bare GCE (A) and the (GQDs–$NHCH_2CH_2NH$)/GCE (B).

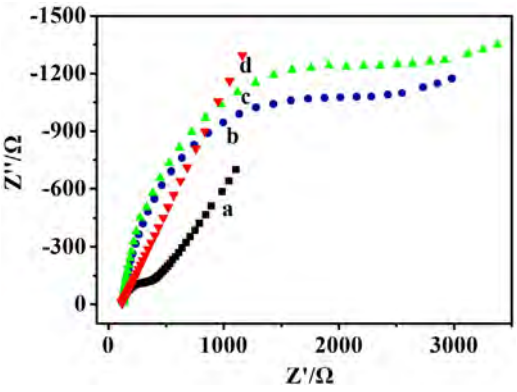

Fig. 3. EIS of the bare GCE (a), carboxylated GCE (b), $NHCH_2CH_2NH$/GCE (c) and the (GQDs–$NHCH_2CH_2NH$)/GCE (d) in 0.1 M KCl electrolyte solution containing 0.1 mM $Fe(CN)_6^{4-/3-}$, the applied ac frequency range: 0.01 Hz to 100 kHz.

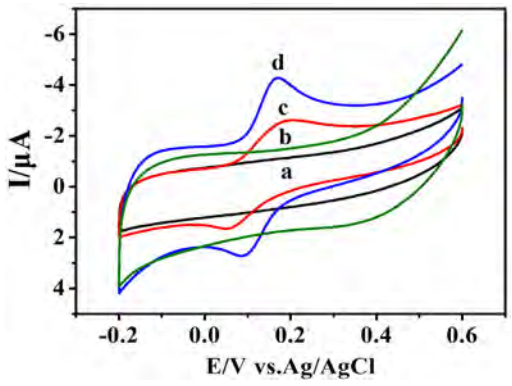

Fig. 4. CVs of the bare GCE (a), (c) and the (GQDs–$NHCH_2CH_2NH$)/GCE (b), (d) in 0.1 M pH 7.0 PBS without and with 0.1 mM DA respectively, scan rate: 100 mV s^{-1}.

maximum at 2.0 mg/mL, and then decreased weakly. Therefore, the 2.0 mg/mL was selected as an optimal concentration for the preparation of the (GQDs–$NHCH_2CH_2NH$)/GCE in the following experiments.

3.4. Different scan rates to the electrochemical redox of DA

In order to investigate the electrochemical process of DA on the (GQDs–$NHCH_2CH_2NH$)/GCE, the effect of different scan rates on the voltammetric response to DA were studied in detail. Fig. 6A shows the CVs of the (GQDs–$NHCH_2CH_2NH$)/GCE in 0.1 M pH 7.0 PBS with 0.1 mM DA at different scan rates. It is clearly observed that both the oxidation and reduction peak currents increase with increasing the scan rates. As shown in Fig. 6B, the redox peak currents of DA increase linearly with the square root of the scan rates in the range of 0.02–0.3 V s^{-1}, the regression equations are $I_{pa} = -(14.4 \pm 0.2)\ v^{1/2} - (0.013 \pm 0.003)$(μA, $mV^{1/2}\ s^{1/2}$, R = 0.990) and $I_{pc} = -(15.9 \pm 0.3)\ v^{1/2} - (2.3 \pm 0.02)$(μA, $mV^{1/2}\ s^{1/2}$, R = 0.990). This suggests that the redox of DA on the (GQDs–$NHCH_2CH_2NH$)/GCE is a diffusion-controlled process [19].

3.5. pH effect

The electrochemical behavior of DA on the (GQDs–$NHCH_2CH_2NH$)/GCE in 0.1 M PBS containing 0.1 mM DA with different pH values (from 5.0 to 9.0) was also investigated by CVs, as shown in Fig. 7A. The oxidation and reduction peak potentials shift negatively with increasing the pH value. Furthermore, there is a good linear relationship between E_{pa}, E_{pc} and pH value (Fig. 7B). The regression equations can be expressed as $E_{pc} = -(0.041 \pm 0.003)$ pH + (0.379 ± 0.020) (R = −0.992) and $E_{pa} = -(0.050$ pH $\pm 0.004) + (0.505 \pm 0.030)$(R = −0.987), indicating the proton involved in the redox reaction. According to the formula: $dE_p / dpH = 2.303$ mRT/nF, in which m is the number of proton and n is the number of electron, the E_{pa} slope value was −0.050, m/n was calculated to be 0.84 for the oxidation process, which shows that the number of proton and electron involving in the electrochemical redox process of DA is equal [30]. Therefore, the possible reaction process of DA on the (GQD–$NHCH_2CH_2NH$)/GCE was described as Scheme 2.

3.6. Analytical application of the (GQDs–$NHCH_2CH_2NH$)/GCE to DA

The (GQDs–$NHCH_2CH_2NH$)/GCE was used for the detection DA by the DPVs under optimal conditions. As shown in Fig. 8, the oxidation peak currents increase with the increasing of the DA concentrations. The oxidation peak current of DA linearly increases with its concentration from 1 to 150 μM (inset in Fig. 8), and the linear regression equation is I_{pa}(μA) = −(0.093 ± 0.002) C (μM) − (5.42 ± 0.02)(R = −0.996). The detection limit is estimated to be 0.115 μM based on the signal-to-noise ratio of 3 and the sensitivity is estimated to 1306 μA $mM^{-1}\ cm^{-2}$. It is observed that the detection limit linear range and the sensitivity in our work is superior to the other reported DA sensors, such as the GO/GCE [27], the GQD/GCE [28], and the Gs-DMF/GCE [29], which are summed up in Table 1. The superiority of the (GQDs–$NHCH_2CH_2NH$)/GCE can be ascribed to the GQDs which possess good electrochemical performance with amounts of oxygen-containing groups and the self-assembled process activates the oxygen groups and protects structure properties of GQDs from damaging.

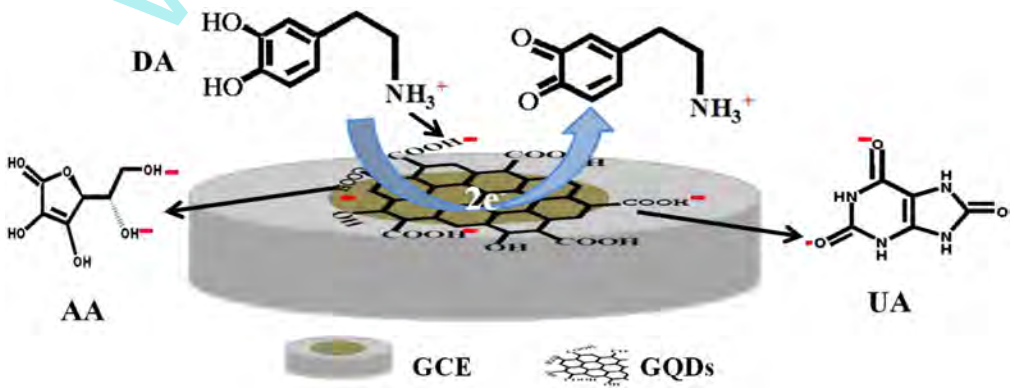

Scheme 1. The schematic illustration of the reaction mechanism of DA on the GQDs–$NHCH_2CH_2NH$/GCE.

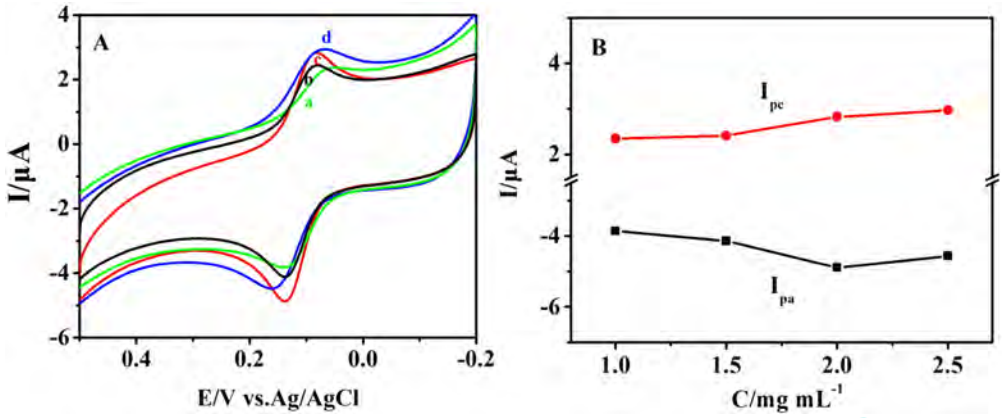

Fig. 5. (A) CVs of the (GQDs–$NHCH_2CH_2NH$)/GCE containing different GQDs concentrations (a–d: 1.0, 1.5, 2.0, 2.5) in 0.1 M pH 7.0 PBS with 0.10 mM DA, (B) plots of the oxidation and reduction peak currents and the GQDs concentrations.

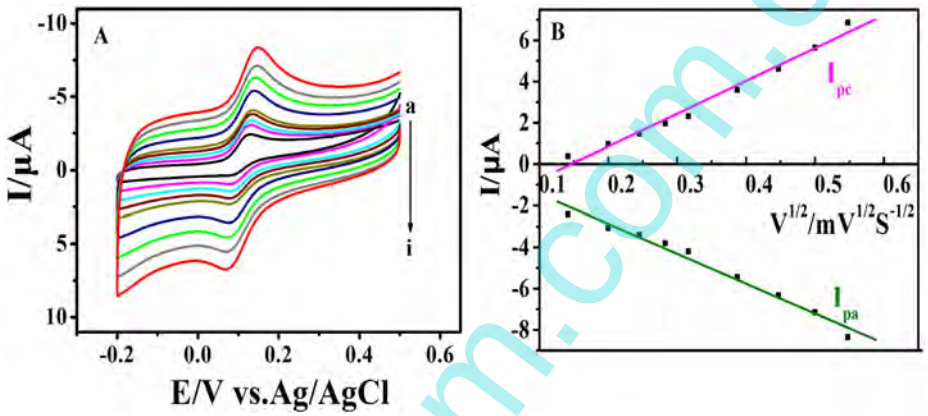

Fig. 6. (A) CVs of the (GQDs–$NHCH_2CH_2NH$)/GCE in 0.1 M pH 7.0 PBS containing 0.10 mM DA at different scan rates (a–i: 0.02, 0.04, 0.06, 0.08, 0.10, 0.15, 0.20, 0.25, 0.30 V s^{-1}), (B) plots of the oxidation and reduction peak currents and the square root of the scan rate.

3.7. Anti-interference property, reproducibility and stability of the (GQDs–$NHCH_2CH_2NH$)/GCE

As we all known the oxidation peak potentials of UA, AA and DA are very close at bare GCE, so their compounds are very difficult to separate due to their overlapping signals [34]. Fig. 9 displays the DPVs of the (GQDs–$NHCH_2CH_2NH$)/GCE to successive additions of 0.1 mM AA, DA and UA in 0.1 M pH 7.0 PBS. Their oxidation peak potentials appear at −0.192, 0.096 and 0.287 V respectively, which can be ascribed to the oxidizing of AA, DA and UA, respectively. The peak-to-peak separation is 0.288 V and 0.194 V, which are large enough to avoid the interference of AA and UA for the determination of DA at the (GQDs–$NHCH_2CH_2NH$)/GCE. This can be ascribed to that both AA (pKa = 4.1) and UA (pKa = 5.75) are negatively charged, and DA (pKa = 8.89) is positively charged in the pH 7.0 PBS. Besides the GQDs have negative carboxyl groups, which selectively attracts cationic DA and prevents anionic AA and UA from reaching the electrode surface. The negatively carboxyl groups of GQDs not only provides good stability but also enables interaction

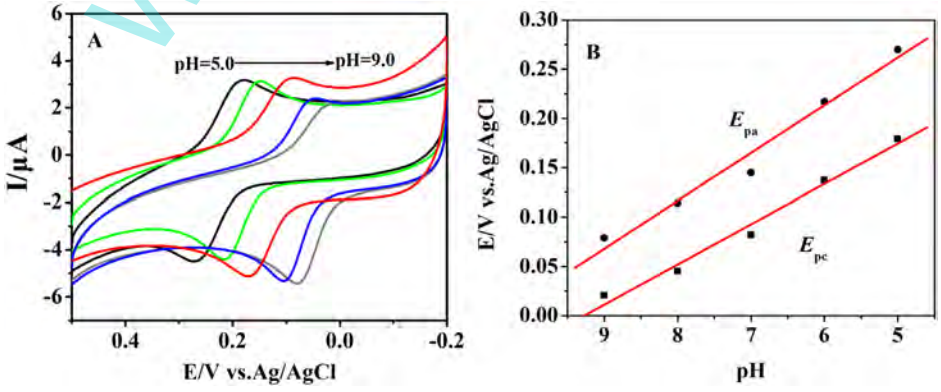

Fig. 7. (A) CVs of the (GQDs–$NHCH_2CH_2NH$)/GCE in 0.1 M pH 7.0 PBS containing 0.10 mM DA with pH range from 5.0 to 9.0; (B) the relationship between the oxidation and reduction peak potentials and the solution pH.

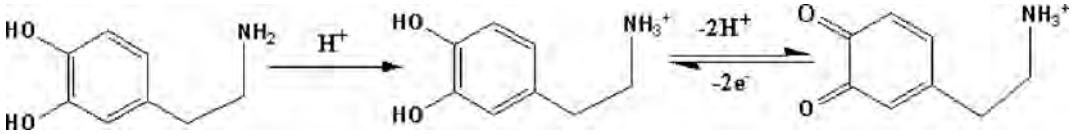

Scheme 2. The reaction process of DA on the (GQD–$NHCH_2CH_2NH$)/GCE.

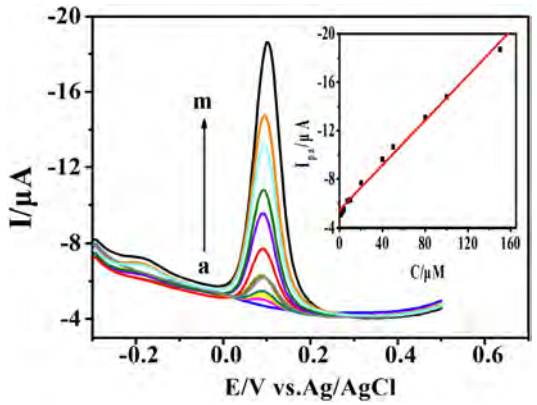

Fig. 8. DPVs of the (GQDs–$NHCH_2CH_2NH$)/GCE in 0.1 M pH 7.0 PBS containing different concentrations of DA (from bottom to up 0, 1, 2, 3, 4, 7, 10, 20, 40, 50, 80, 100 and 150 μM); Inset: plot of oxidation peak currents and DA concentrations.

with the amine functional groups in DA through electrostatic interaction to recognize DA with high selectivity [9]. Furthermore, other influences from common co-existing substances were also investigated. It is found that most ions and common substances at high concentration only cause negligible change: K^+, Cl^-, NO_3^-, SO_4^{2-} (>300 fold), Ca^{2+}, Zn^{2+}, Mg^{2+}, (150 fold), H_2O_2, citric acid, fructose, mannose, and ethanol, lysine, cysteine and glucose (100 fold). The results indicate that (GQDs–$NHCH_2CH_2NH$)/GCE exhibits good selectivity for DA detection.

Reproducibility and stability are two important parameters for electrochemical sensors. In this work, the fabrication reproducibility for six (GQDs–$NHCH_2CH_2NH$)/GCEs was investigated by comparing their current responses to 0.1 mM DA. The calculated result shows that the relative standard deviation (RSD) is 3.78%, which is an acceptable reproducibility. The stability of the (GQDs–$NHCH_2CH_2NH$)/GCE was checked after it was stored in room temperature for one month. The current response decreases 4.5% than the initial response, indicating a wonderful stability.

3.8. Application of the DA sensor in real samples

In order to evaluate the validity of the proposed DA sensor, the analytical application was carried out by DPV to determination DA in Dopamine Hydrochloride Injection. As shown in Table 2, the recoveries of the different Dopamine Hydrochloride Injection concentrations are in the range from 97.8% to 99.6%. As AA, UA often coexists with DA in the blood samples, and the oxidation peak potentials of UA, AA, and DA are very close. Therefore, to simulate the vivo samples, the concentrations of 20 μM, 30 μM and 40 μM AA and UA were added to 40 μM DA injection solutions, the obtained DPV results of the DA recovery rate of the samples were 96.8%, 97.0% and 95.9% respectively, which demonstrate satisfactory results in real samples determination. The above results prove that the DA sensor has a great potential in practical applications.

Table 1
Comparison of the analytical performance between the (GQDs–$NHCH_2CH_2NH$)/GCE and different modified electrodes.

Modified materials	Sensitivity ($\mu A\ mM^{-1}\ cm^{-2}$)	Linear range (μM)	Detection limit (μM)	References
GEM	928	4.0–100	2.64	[31]
Tyrosinase/BDD	68.6	5.0–120	1.3	[32]
Tyrosinase/egg shell/membrane	10.6	50–250	25	[33]
Tyrosinase-SWNTs-Ppy/GCE	467	5–50	5	[13]
NPG/Au	–	1.5–27.5	1.5	[35]
Laccase/SiO_2-PA/GCE	392	0.99–103.1	0.26	[36]
(GQDs–$NHCH_2CH_2NH$)/GCE	1306	1.0–150	0.115	This work

Note: GEM: graphene modified electrode; BDD: boron-doped diamond electrode; SWNTs: single wall carbon nanotubes; Ppy: polypyrrole; NPG: nanoporous gold nanofilm; PA: phytic acid; GQDs: graphene quantum dots.

4. Conclusions

In this study, we have developed a stable GQDs modified electrode via covalent monolayers self-assembly method using ethylenediamine as arm linker. The obtained (GQDs–$NHCH_2CH_2NH$)/GCE presents good electrochemical redox behavior to DA and can be used for the determination of DA. Under the selected conditions, the DPV oxidation peak currents of the (GQDs–$NHCH_2CH_2NH$)/GCE shows good linear relationship with DA concentration in the range from 1 to 150 μM with the low detection limit of 0.115 μM and the well sensitivity of 1306 $\mu A\ mM^{-1}\ cm^{-2}$. The DA sensor also has strong anti-interference to some potential interfering substances such as AA, UA. In addition, it also displays well reproducibility and stability.

Acknowledgments

This work was supported by the National Natural Science Foundation of China (No. 21175115), the Program for New Century Excellent

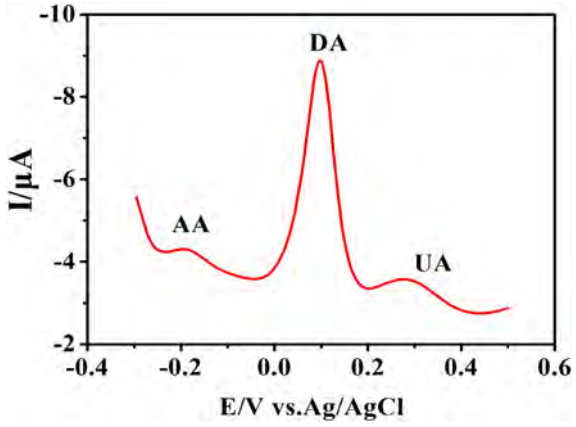

Fig. 9. DPV of the (GQDs–$NHCH_2CH_2NH$)/GCE in 0.1 M pH 7.0 PBS containing 0.1 mM AA, DA and UA.

Table 2
Determination of DA in Dopamine Hydrochloride Injection with the sensor.

Samples	Added (μM)	Found (μM)	Recovery (%)
1	20	19.64	98.2
2	40	39.12	97.8
3	60	59.75	99.6

Talents in Minnan Normal University (MX14003), and the Innovation Base Foundation for Graduate Students Education of Fujian Province.

References

[1] J. Njagi, M.M. Chernov, J.C. Leiter, S. Andreescu, Anal. Chem. 82 (2010) 989–996.
[2] A. Abbaspour, A. Khajehzadeh, A. Ghaffarinejad, Analyst 134 (2009) 1692–1698.
[3] Y. Lin, C. Chen, C. Wang, F. Pu, J. Ren, X. Qu, Chem. Commun. 47 (2011) 1181–1183.
[4] V. Carrera, E. Sabater, E. Vilanova, M.A. Sogorb, J. Chromatogr. B 847 (2007) 88–94.
[5] M. Liu, Q. Chen, C. Lai, Y. Zhang, J. Deng, H. Li, S. Yao, Biosens. Bioelectron. 48 (2013) 75–81.
[6] E. Canbay, E. Akyilmaz, Anal. Biochem. 444 (2014) 8–15.
[7] Z.-H. Sheng, X.-Q. Zheng, J.-Y. Xu, W.-J. Bao, F.-B. Wang, X.-H. Xia, Biosens. Bioelectron. 34 (2012) 125–131.
[8] W. Zhang, R. Yuan, Y.-Q. Chai, Y. Zhang, S.-H. Chen, Sensors Actuators B 166 (2012) 601–607.
[9] Q. Huang, S. Hu, H. Zhang, J. Chen, Y. He, F. Li, W. Weng, J. Ni, X. Bao, Y. Lin, Analyst 138 (2013) 5417–5423.
[10] C. Xiao, X. Chu, Y. Yang, X. Li, X. Zhang, J. Chen, Biosens. Bioelectron. 26 (2011) 2934–2939.
[11] H. Zhu, W. Wu, H. Zhang, L. Fan, S. Yang, Electroanalysis 21 (2009) 2660–2666.
[12] Y. Li, L. Zhang, M. Li, Z. Pan, D. Li, Chem. Cent. J. 6 (2012) 103.
[13] K. Min, Y.J. Yoo, Talanta 80 (2009) 1007–1011.
[14] X. Zhou, P. Ma, A. Wang, C. Yu, T. Qian, S. Wu, J. Shen, Biosens. Bioelectron. 64 (2015) 404–410.
[15] S. Zhu, J. Zhang, C. Qiao, S. Tang, Y. Li, W. Yuan, B. Li, L. Tian, F. Liu, R. Hu, Chem. Commun. 47 (2011) 6858–6860.
[16] J. Shen, Y. Zhu, X. Yang, C. Li, Chem. Commun. 48 (2012) 3686–3699.
[17] L.-s. Li, X. Yan, J. Phys. Chem. Lett. 1 (2010) 2572–2576.
[18] J. Peng, W. Gao, B.K. Gupta, Z. Liu, R. Romero-Aburto, L. Ge, L. Song, L.B. Alemany, X. Zhan, G. Gao, S.A. Vithayathil, B.A. Kaipparettu, A.A. Marti, T. Hayashi, J.-J. Zhu, P.M. Ajayan, Nano Lett. 12 (2012) 844–849.
[19] L. Tang, R. Ji, X. Cao, J. Lin, H. Jiang, X. Li, K.S. Teng, C.M. Luk, S. Zeng, J. Hao, ACS Nano 6 (2012) 5102–5110.
[20] C. Zhou, W. Jiang, B.K. Via, Colloids Surf. B 118 (2014) 72–76.
[21] J. Zhao, G. Chen, L. Zhu, G. Li, Electrochem. Commun. 13 (2011) 31–33.
[22] H. Razmi, R. Mohammad-Rezaei, Biosens. Bioelectron. 41 (2013) 498–504.
[23] J.-J. Liu, Z.-T. Chen, D.-S. Tang, Y.-B. Wang, L.-T. Kang, J.-N. Yao, Sensors Actuators B 212 (2015) 214–219.
[24] Y. Zhang, C. Wu, X. Zhou, X. Wu, Y. Yang, H. Wu, S. Guo, J. Zhang, Nanoscale 5 (2013) 1816–1819.
[25] R.R. Costa, A.M. Testera, F.J. Arias, J.C. Rodríguez-Cabello, J.F. Mano, J. Phys. Chem. B 117 (2013) 6839–6848.
[26] L. Su, F. Gao, L. Mao, Anal. Chem. 78 (2006) 2651–2657.
[27] S.W. Lee, B.-S. Kim, S. Chen, Y. Shao-Horn, P.T. Hammond, J. Am. Chem. Soc. 131 (2008) 671–679.
[28] Y. Dong, J. Shao, C. Chen, H. Li, R. Wang, Y. Chi, X. Lin, G. Chen, Carbon 50 (2012) 4738–4743.
[29] C. Hu, Y. Liu, Y. Yang, J. Cui, Z. Huang, Y. Wang, L. Yang, H. Wang, Y. Xiao, J. Rong, J. Mater. Chem. B 1 (2013) 39–42.
[30] C.R. Raj, T. Ohsaka, J. Electroanal. Chem. 496 (2001) 44–49.
[31] Y.-R. Kim, S. Bong, Y.-J. Kang, Y. Yang, R.K. Mahajan, J.S. Kim, H. Kim, Biosens. Bioelectron. 25 (2010) 2366–2369.
[32] Y.L. Zhou, R.H. Tian, J.F. Zhi, Biosens. Bioelectron. 22 (2007) 822–828.
[33] S. Tembe, B.S. Kubal, M. Karve, S.F. D'Souza, Anal. Chem. Acta 612 (2008) 212–217.
[34] L. Liu, S. Li, L. Liu, D. Deng, N. Xia, Analyst 137 (2012) 3794–3799.
[35] P.-Y. Ge, Y. Du, J.-J. Xu, H.-Y. Chen, J. Electroanal. Chem. 633 (2009) 182–186.
[36] K. Wang, P. Liu, Y. Ye, J. Li, W. Zhao, X. Huang, Sensors Actuators B 197 (2014) 292–299.